

Fidelity approach to quantum phase transitions in quantum Ising model

Bogdan Damski

Jagiellonian University, Institute of Physics, Łojasiewicza 11, 30-348 Kraków, Poland

Fidelity approach to quantum phase transitions uses the overlap between ground states of the system to gain some information about its quantum phases. Such an overlap is called fidelity. We illustrate how this approach works in the one dimensional quantum Ising model in the transverse field. Several closed-form analytical expressions for fidelity are discussed. An example of what insights fidelity provides into the dynamics of quantum phase transitions is carefully described. The role of fidelity in central spin systems is pointed out.

Proceedings of the 50th Karpacz Winter School of Theoretical Physics, Karpacz, Poland, 2-9 March 2014

I. INTRODUCTION

Quantum phase transitions happen when small variations of an external parameter fundamentally change the ground state properties of the system [1, 2]. They typically appear when there are competing interactions trying to order the sample in different ways and the balance between them is controlled by an external field.

The fidelity approach to quantum phase transitions uses the overlap between ground states to gain some information about the quantum phases [3, 4]. For example, we can define fidelity as

$$F(g, \delta) = |\langle g - \delta | g + \delta \rangle|, \quad (1)$$

where we assumed that the Hamiltonian \hat{H} of the system depends on some parameter g (e.g. an external field whose variation induces a quantum phase transition), $|g\rangle$ stands for the non-degenerate ground state of the Hamiltonian $\hat{H}(g)$, and δ is a parameter shift. Besides depending on g and δ , fidelity also depends on N , i.e., the size of the system (number of spins, atoms, etc.).

The fidelity approach to quantum phase transitions is based on the expectation that fidelity should exhibit a marked drop near the critical point, where the ground states of the Hamiltonian are most sensitive to the external field. Fidelity has been studied in the following limits:

- $\delta \rightarrow 0$ at the fixed system size N : one employs here the Taylor expansion to get

$$F(g, \delta) = 1 - 2\chi(g)\delta^2 + \mathcal{O}(\delta^4), \quad (2)$$

where the linear in δ term disappears due to the normalization condition $\langle g | g \rangle = 1$. Alternatively, one may note that such a term could make $F(g, \delta) > 1$ or that it would break the $\delta \rightarrow -\delta$ symmetry of $F(g, \delta)$. The central object of this expansion is the fidelity susceptibility $\chi(g)$. Using the scaling theory of quantum phase transitions [1, 5], it has been shown that at the critical point g_c in a d dimensional system [6, 7]

$$\chi(g_c) \sim N^{2/d\nu}, \quad (3)$$

while far away from it

$$\chi(g) \sim \frac{N}{|g - g_c|^{2-d\nu}}, \quad (4)$$

where ν is the universal critical exponent describing the divergence of the correlation length $\xi(g)$ near the critical point, $\xi(g) \sim |g - g_c|^{-\nu}$. Fidelity susceptibility can be viewed in two ways. First, it can be treated as a function whose knowledge leads to the determination of fidelity (1) through Eq. (2). One should remember, however, that it can be used in such a way only when the $\mathcal{O}(\delta^4)$ term is negligible, which sets conditions on the system size N , the distance from the critical point $|g - g_c|$, and the field shift δ . For example, the expansion (2) always breaks for large enough systems. Second, one can formally define fidelity susceptibility through the relation

$$\chi(g) = - \left\langle g \left| \frac{d^2}{dg^2} \right| g \right\rangle, \quad (5)$$

and use it to study the quantum phase transitions for any system size N and any parameter g (see e.g. Refs. [8–10], where fidelity susceptibility gives the diagonal elements of the geometric tensor providing some information about the quantum critical points). Finally, we mention that it has been recently proposed that fidelity susceptibility can be extracted out from the spectral function [11], which can be measured in standard condensed matter setups.

- $N \rightarrow \infty$ at the fixed field shift δ : this is the limit, where the Anderson orthogonality catastrophe [12], i.e., the disappearance of the overlap between ground states of the thermodynamically large system, happens. We have argued that at the critical point [13]

$$\frac{\ln F(g_c, \delta)}{N} \sim -|\delta|^{d\nu}, \quad (6)$$

while far away from it

$$\frac{\ln F(g, \delta)}{N} \sim -\frac{\delta^2}{|g - g_c|^{2-d\nu}} \quad (7)$$

as long as $d\nu < 2$. Eq. (7) becomes equivalent to Eq. (4) when $N\delta^2/|g - g_c|^{2-d\nu} \ll 1$. We mention that $-\ln F/N$ is called fidelity per lattice site [14, 15].

The outline of these lecture notes is the following. Sec. II presents basic concepts associated with the quantum Ising model. The main stress in this section is placed on the discussion of the parity of the ground state of the Ising chain. In Sec. III, we discuss the exact closed-form expression for fidelity susceptibility of the Ising model. Sec. IV is devoted to the studies of fidelity in thermodynamically large systems. We show there how the Anderson orthogonality catastrophe happens in the Ising chain. Sec. V focuses on the dynamics of quantum phase transitions. We explain there how fidelity can be used to obtain the probability of finding the system in the ground state after the non-equilibrium crossing of the quantum critical point. Finally, we briefly discuss in Sec. VI two problems associated with the central spin coupled to the Ising chain. Their solution also involves fidelity.

II. QUANTUM ISING MODEL

The Hamiltonian of the one dimensional quantum Ising model in the transverse field reads

$$\hat{H}(g) = -\sum_{i=1}^N (\sigma_i^x \sigma_{i+1}^x + g\sigma_i^z), \quad (8)$$

where g stands for an external magnetic field acting on the system and N is the number of spins. The periodic boundary conditions are assumed, i.e., $\sigma_{N+1}^x = \sigma_1^x$. While the spin-spin interactions in this model try to align the spins in the $\pm x$ direction, the magnetic field tries to put the spins along its direction, i.e., $+z$ for $g > 0$ and $-z$ for $g < 0$. The competition between different spin orientations results in the quantum phase transition between the ferromagnetic and paramagnetic phases (Fig. 1). The system is in the ferromagnetic phase for $|g| < 1$, it is in the paramagnetic phase for $|g| > 1$, and it is at the quantum critical point when $|g| = 1$, i.e., $g_c = \pm 1$. The experimental possibilities for the studies of this model and other Ising-like models appear in cobalt niobate [16], as well as in cold ion [17, 18], cold atom [19], and NMR [20] simulators of spin systems.

This model is exactly solvable [21–23]. Its role in the studies of strongly correlated quantum systems parallels the role of the harmonic oscillator in the single-particle quantum theory: Numerous theoretical concepts in many-body quantum physics are being tested in the quantum Ising chain in the transverse field.

To correctly compute fidelity of the quantum Ising model, one has to properly identify the parity symmetry of its ground state [6, 24]. We will follow below the discussion from Ref. [24], where the comprehensive study of this problem in a *finite* Ising chain is presented (see also Ref. [25] for the discussion of the finite-size effects in the XY model).

First, we note that the Hamiltonian (8) commutes with the parity operator

$$[\hat{H}, \hat{P}] = 0, \quad \hat{P} = \prod_{i=1}^N \sigma_i^z,$$

whose eigenvalues are either $+1$ or -1 . Thus, the Hamiltonian (8) can be independently diagonalized in the positive and negative parity subspaces.

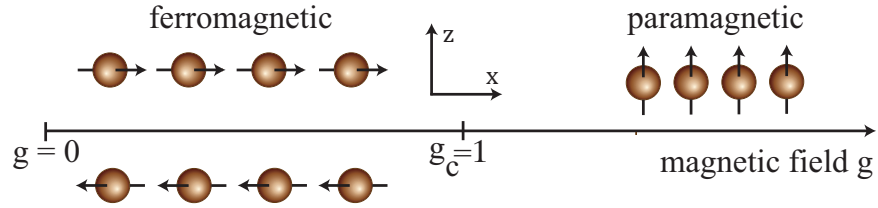


Figure 1: Schematic illustration of the quantum phase transition in the quantum Ising model. Adapted from Ref. [26].

Second, one performs the Jordan-Wigner transformation mapping the spin-1/2 operators to fermionic operators

$$\sigma_i^z = 1 - 2\hat{c}_i^\dagger \hat{c}_i, \quad \sigma_i^x = (\hat{c}_i + \hat{c}_i^\dagger) \prod_{j<i} (1 - 2\hat{c}_j^\dagger \hat{c}_j), \quad \{\hat{c}_i, \hat{c}_j^\dagger\} = \delta_{ij}, \quad \{\hat{c}_i, \hat{c}_j\} = 0.$$

Substituting this into Eq. (8), one obtains

$$\hat{H}(g) = - \sum_{i=1}^N \left[\hat{f}_{i,i+1} + g (\hat{c}_i \hat{c}_i^\dagger - \hat{c}_i^\dagger \hat{c}_i) \right], \quad (9)$$

$$\hat{f}_{i,j} = \hat{c}_i^\dagger \hat{c}_j - \hat{c}_i \hat{c}_j^\dagger - \hat{c}_i \hat{c}_j + \hat{c}_i^\dagger \hat{c}_j^\dagger,$$

where

$$\hat{c}_{N+1} = -\hat{c}_1 \quad (10)$$

should be taken in the positive parity subspace and

$$\hat{c}_{N+1} = \hat{c}_1 \quad (11)$$

in the negative parity subspace. Since the Hamiltonian (9) is quadratic in the fermionic operators, it can be diagonalized in the standard way. One first substitutes

$$\hat{c}_j = \frac{\exp(-i\pi/4)}{\sqrt{N}} \sum_{K=\pm k} \hat{c}_K \exp(iKj) \quad (12)$$

into the Hamiltonian (9), where[48]

$$k = \frac{\pi}{N}, \frac{3\pi}{N}, \frac{5\pi}{N}, \dots, \pi - \frac{\pi}{N} \quad \text{for even } N, \quad (13)$$

$$k = \frac{\pi}{N}, \frac{3\pi}{N}, \frac{5\pi}{N}, \dots, \pi \quad \text{for odd } N,$$

in the positive parity subspace and

$$k = 0, \frac{2\pi}{N}, \frac{4\pi}{N}, \dots, \pi \quad \text{for even } N, \quad (14)$$

$$k = 0, \frac{2\pi}{N}, \frac{4\pi}{N}, \dots, \pi - \frac{\pi}{N} \quad \text{for odd } N,$$

in the negative parity subspace. The quantization of momenta (13) and (14) follows from the boundary conditions (10) and (11), respectively. Then one performs the standard Bogolubov transformation to diagonalize the resulting Hamiltonian.

Third, one needs to determine whether the ground state of the Ising Hamiltonian (8) lies in the positive or negative parity subspace. This can be done by computing the lowest eigenenergy in each of the subspaces, say ε^+ and ε^- in the positive and negative parity subspaces, respectively. We find that $\varepsilon^- - \varepsilon^+$ equals [24]

$$g^N \int_0^1 dt \frac{4N t^{N-3/2} \sqrt{(1-t)(1-g^2t)}}{\pi (1-(gt)^{2N}}$$

in the ferromagnetic phase,

$$\text{sign}(g^N)(2|g| - 2) + g^{-N} \int_0^1 dt \frac{4N t^{N-3/2} \sqrt{(1-t)(g^2-t)}}{1-t^{2N}/g^{2N}}$$

in the paramagnetic phase, and

$$2 \tan\left(\frac{\pi}{4N}\right) \text{sign}(g_c^N)$$

at the critical points.

A quick look at these expressions shows that the parity of the ground state of the Hamiltonian (8) is

- positive for all magnetic fields when the number of spins N is even,
- positive for $g > 0$ and negative for $g < 0$ in the odd-sized systems.

These remarks follow from the observation that $\text{sign}(\varepsilon^- - \varepsilon^+) = \text{sign}(g^N)$. The same result was obtained in a different way in Ref. [6] for $g > 0$.

Besides providing the parity of the ground state, these expressions quantify the gap between the eigenenergies of the positive and negative parity ground states of the Hamiltonian (8):

- *Ferromagnetic phase* ($|g| < 1$). The gap is exponentially small in the thermodynamically large systems

$$|\varepsilon^- - \varepsilon^+| = \mathcal{O}\left(\exp(-N/\xi(g))/\sqrt{N}\right),$$

where

$$\xi(g) = 1/|\ln|g|| \quad (15)$$

is the correlation length of the *infinite* Ising chain [27] and we define the thermodynamic limit by the relation

$$N \gg \xi(g). \quad (16)$$

In the opposite limit,

$$N \ll \xi(g),$$

we find that the gap is polynomial in the system size

$$|\varepsilon^- - \varepsilon^+| = \mathcal{O}(1/N).$$

- *Paramagnetic phase* ($|g| > 1$). The gap is always macroscopic and grows approximately linearly with the distance from the critical point.
- *Critical points* $|g| = 1$. The gap is inversely proportional to the size of the system in large systems.

At the risk of stating the obvious, we mention that the *qualitative* content of these remarks is discussed in textbooks on quantum phase transitions (see e.g. Ref. [1]).

III. FIDELITY SUSCEPTIBILITY OF QUANTUM ISING MODEL

Our discussion in this section will be based on Refs. [26] and [24]. The former one provides the exact closed-form expression for fidelity susceptibility of even-sized Ising chains and studies its basic properties. The latter one generalizes this result to the odd-sized chains and discusses the pitfalls of incorrect identification of the parity of the ground state in fidelity susceptibility computations.

The ground state wave-function of the Ising chain can be written as

$$|g\rangle = \prod_k \left(\cos\left(\frac{\theta_k}{2}\right) - \sin\left(\frac{\theta_k}{2}\right) \hat{c}_k^\dagger \hat{c}_{-k}^\dagger \right) |\text{vac}\rangle, \quad (17)$$

$$\sin(\theta_k) = \frac{\sin(k)}{\sqrt{g^2 - 2g \cos(k) + 1}}, \quad \cos(\theta_k) = \frac{g - \cos(k)}{\sqrt{g^2 - 2g \cos(k) + 1}},$$

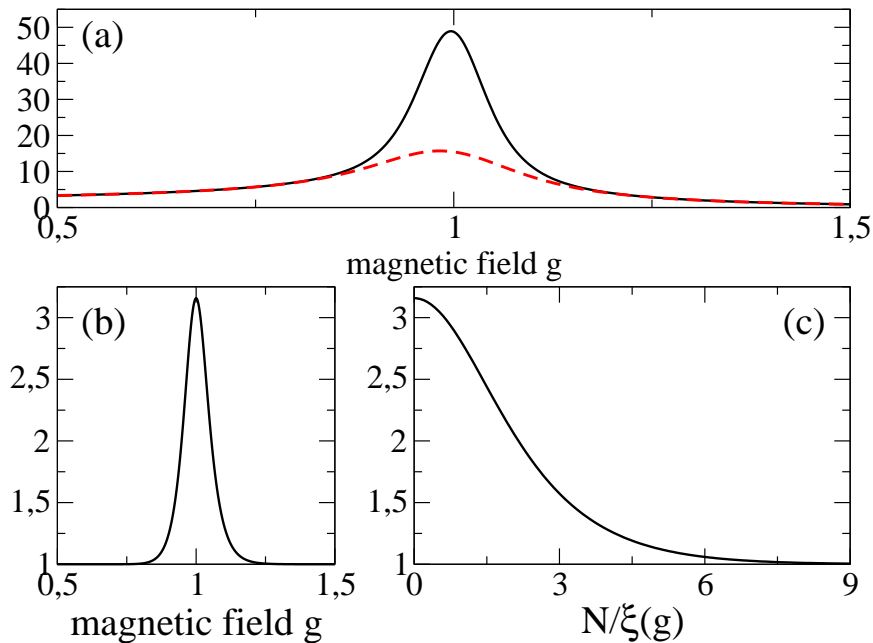


Figure 2: Panel (a): black solid line shows χ^+ (19), while the red dashed line shows χ^- (20). Even $N = 40$ is used. Panel (b): The χ^+/χ^- ratio for data from the (a) panel. Panel (c): the same as panel (b), but as a function of the ratio between the system size and the correlation length $N/\xi(g) = N |\ln|g||$.

where the proper momenta k have to be used: (13) if the ground state of the Hamiltonian (8) lies in the positive parity subspace and (14) if it belongs to the negative parity subspace (see Ref. [24] for the discussion of the $k = 0, \pi$ modes that do not contribute to the following calculations). The $|\text{vac}\rangle$ state is annihilated by all \hat{c}_k operators.

Using this wave-function one easily finds with Eq. (5) that

$$\chi(g) = \frac{1}{4} \sum_k \left(\frac{d\theta_k}{dg} \right)^2 = \frac{1}{4} \sum_k \frac{\sin^2(k)}{(g^2 - 2g \cos(k) + 1)^2}. \quad (18)$$

This summation has been analytically performed in Refs. [24] and [26].

Before providing the definite closed-form expression for fidelity susceptibility, we emphasize the need for the correct identification of the parity of the ground state [24]. If we use the momenta (13) to compute the series (18), we will obtain

$$\chi^+(g) = \frac{N^2}{16g^2} \frac{g^N}{(g^N + 1)^2} + \frac{N}{16g^2} \frac{g^N - g^2}{(g^N + 1)(g^2 - 1)}. \quad (19)$$

If we, however, sum the series (18) over momenta (14), we will get

$$\chi^-(g) = -\frac{N^2}{16g^2} \frac{g^N}{(g^N - 1)^2} + \frac{N}{16g^2} \frac{g^N + g^2}{(g^N - 1)(g^2 - 1)}. \quad (20)$$

These two expressions are plotted in Fig. 2a. They differ negligibly away from the critical point, i.e., for magnetic fields g such that $N \gg \xi(g)$. On the other hand, near the critical point, i.e., for magnetic fields g such that the system size N is smaller than a few correlation lengths $\xi(g)$, they substantially differ (Fig. 2c). This difference was numerically studied in Ref. [6], where it caused problems in the Quantum Monte Carlo studies of fidelity susceptibility at non-zero temperature. Our expressions analytically quantify this difference in the zero temperature limit. For example,

- right at the critical point $g_c = 1$ the ratio of the two expressions equals

$$\left. \frac{\chi^+}{\chi^-} \right|_{g_c=1} = 3 \frac{N}{N-2},$$

and so it approaches 3 as N increases (Figs. 2b and 2c),

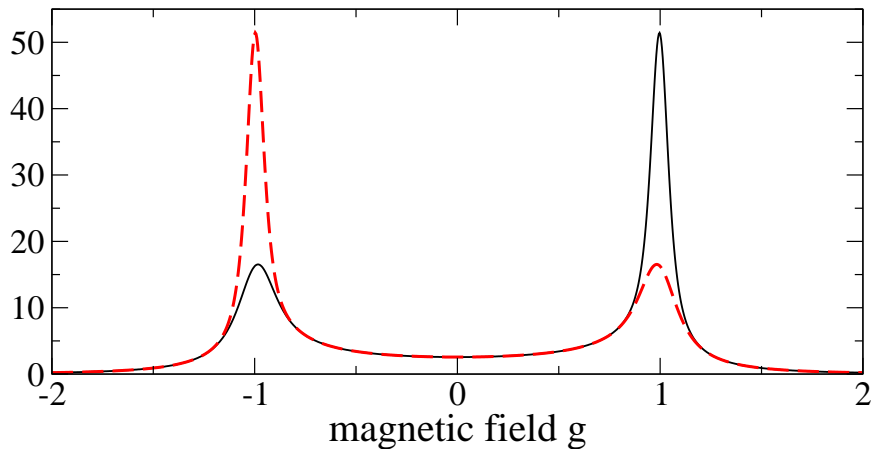


Figure 3: Black solid line shows χ^+ (19), while the red dashed line shows χ^- (20). The plot is done for odd $N = 41$.

- in odd-sized systems neither of the two expressions, (19) and (20), is symmetric with respect to the $g \leftrightarrow -g$ transformation (Fig. 3).

Using the proper identification of the parity of the ground state discussed in Sec. II, one quickly finds that (i) $\chi(g) = \chi^+(g)$ for all system sizes and $g > 0$; (ii) $\chi(g) = \chi^+(g)$ for even-sized systems and $g < 0$; and (iii) $\chi(g) = \chi^-(g)$ for odd-sized systems and $g < 0$. Correlating the observations (i) – (iii) with equations (19) and (20), we get

$$\chi(g) = \frac{N^2}{16g^2} \frac{|g|^N}{(|g|^N + 1)^2} + \frac{N}{16g^2} \frac{|g|^N - g^2}{(|g|^N + 1)(g^2 - 1)}. \quad (21)$$

This exact closed-form expression works for any system size $N \geq 2$ and any magnetic field g . As expected, it is symmetric with respect to the $g \leftrightarrow -g$ transformation. Its properties can be summarized as follows [26].

First, it undergoes a simple transformation law under the Kramers-Wannier duality mapping [28]

$$g \leftrightarrow \frac{1}{g}. \quad (22)$$

Indeed, one easily verifies that [26]

$$g^2 \chi(g) = \left(\frac{1}{g}\right)^2 \chi\left(\frac{1}{g}\right). \quad (23)$$

Second, one finds that away from the critical point in the paramagnetic phase

$$\chi(g) = \frac{N}{16g^2(g^2 - 1)} + R(|g|), \quad (24)$$

where the remainder R , which can be easily computed from Eq. (21), can be shown [26] to be negligible when inequality (16) holds. It should be stressed that the main part of this result can be obtained by replacing the sum by the integral (see e.g. Refs. [4], [7], and [8])

$$\sum_k \rightarrow \frac{N}{2\pi} \int_0^\pi dk \quad (25)$$

in Eq. (18). While such a replacement works well away from the critical point, it leads to a completely wrong result near the critical point. The formal approach to the replacement of the sum by the integral is provided by the Euler-Maclaurin summation formula [29]. For example, adopting this formula to the even N positive parity case, we

get

$$\begin{aligned}
\sum_{k=\pi/N}^{\pi-\pi/N} f(k) &= \frac{N}{2\pi} \int_{\pi/N}^{\pi-\pi/N} dk f(k) \\
&+ \frac{1}{2} \left[f\left(\frac{\pi}{N}\right) + f\left(\pi - \frac{\pi}{N}\right) \right] \\
&+ \sum_{m=1}^{s-1} \frac{(-1)^m B_m}{(2m)!} \left(\frac{2\pi}{N}\right)^{2m-1} \left[f^{(2m-1)}\left(\frac{\pi}{N}\right) - f^{(2m-1)}\left(\pi - \frac{\pi}{N}\right) \right] \\
&- \left(\frac{2\pi}{N}\right)^{2s} \frac{1}{(2s)!} \int_0^1 dt \phi_{2s}(t) \sum_{k=\pi/N}^{\pi-3\pi/N} f^{(2s)}\left(k + t \frac{2\pi}{N}\right),
\end{aligned} \tag{26}$$

where

$$f(k) = \frac{1}{4(g^2 - 2g \cos(k) + 1)^2}, \quad f^{(m)}(k) = \frac{d^m}{dk^m} f(k),$$

an integer $s \geq 1$ is a parameter that can be chosen at will, B_s are Bernoulli numbers, and ϕ_s are the Bernoulli polynomials (we use the convention for B_s and ϕ_s from Ref. [29]). Therefore, by performing (25) one skips the second, third and the fourth line of the right hand side of Eq. (26), and replaces the integration ranges π/N and $\pi - \pi/N$ in the first line by 0 and π , respectively. This procedure is bound to fail near the critical point. A quick inspection of expression (26) shows that the exact computation of the sum (18) is easier than the formal study of the Euler-Maclaurin expression (26)!

Before moving on, we mention that the application of the duality mapping (22) to Eq. (24) provides us with the following expression for fidelity susceptibility in the ferromagnetic phase

$$\chi(g) = \frac{N}{16(1-g^2)} + \frac{R(1/|g|)}{g^4}, \tag{27}$$

where again the remainder is negligible away from the critical point, i.e., when the condition (16) is satisfied.

Third, near the critical point one can expand the exact expression in a series to get [26]

$$\chi(g) = \frac{N(N-1)}{32g^2} \left(1 - \frac{N+1}{N} \frac{(N \ln |g|)^2}{6} + r(|g|) \right),$$

where this time the reminder $r(|g|)$ is negligible for $N \ll \xi(g)$. In particular, at the critical points one finds

$$\chi(g_c) = \frac{N(N-1)}{32}. \tag{28}$$

Fourth, noting that $d = \nu = 1$ and $g_c = \pm 1$ in our quantum Ising model [23], one easily verifies the scaling relations (3) and (4) by comparing them to the equations (24), (27), and (28).

Fifth, one can show from the exact solution (21), that the maximum of fidelity susceptibility is located in the ferromagnetic phase at the distance

$$\frac{6}{N^2} - \frac{6}{N^3} + \mathcal{O}(N^{-4})$$

from the critical point [26]. The fact that the maximum is shifted away from the critical point due to the finite-size effects is not surprising: The shift proportional to $1/N^2$ is expected for free fermionic systems [30]. The shift of the maximum into the ferromagnetic phase is the consequence of the duality symmetry (23), which the reader can easily verify.

IV. FIDELITY IN THERMODYNAMICALLY LARGE ISING CHAIN

Using wave-function (17), one easily finds that

$$\begin{aligned}
F(g, \delta) &= \prod_k \cos\left(\frac{\theta_+(k) - \theta_-(k)}{2}\right), \\
\tan \theta_{\pm}(k) &= \frac{\sin(k)}{g \pm \delta - \cos(k)}.
\end{aligned} \tag{29}$$

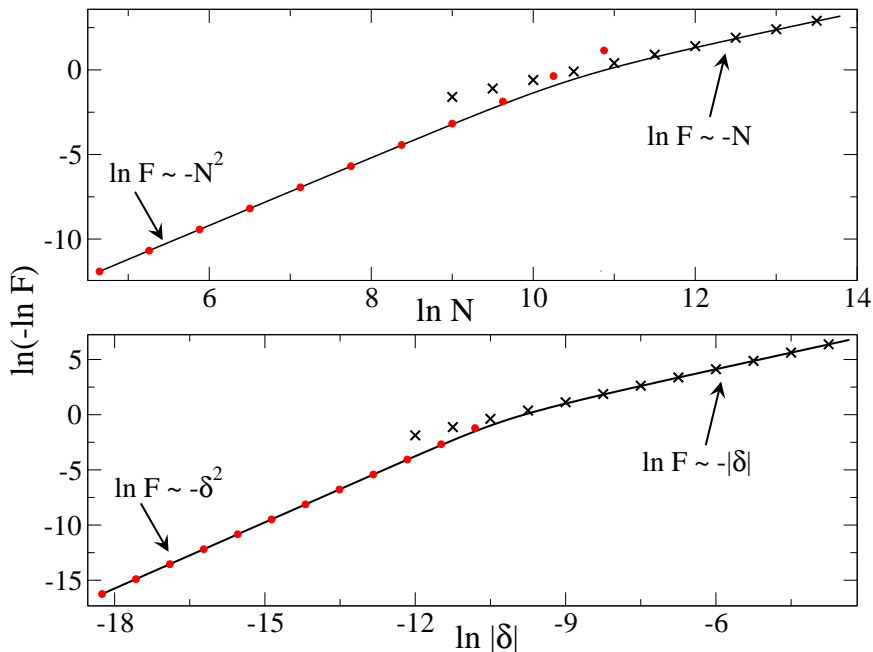


Figure 4: Illustration of the transition to the thermodynamic limit. In both panels the black solid line shows $F(g_c = 1, \delta)$. Upper panel: the field shift $\delta = 10^{-4}$. Lower panel: the system size N is set to 10^5 . Red dots come from $F = 1 - N(N-1)\delta^2/16$, i.e., the approximation of fidelity (2) through fidelity susceptibility (28). The black crosses come from the leading-order thermodynamic approximation (31), which for $g = 1$, i.e., $c = 0$, reads $\ln F = -N|\delta|/4$.

We are now interested in studying this expression in the thermodynamic limit near the critical point $g_c = 1$. In fact, from now on we will focus on $g \geq 0$ and assume even N for convenience. This section is based on our Refs. [13] and [31].

The transition to the thermodynamic limit can be induced by either the change of the system size N or the change of the field shift δ (Fig. 4). It happens in our problem when [13]

$$N \gg \min[(\xi(g + \delta), \xi(g - \delta))].$$

Substituting $\xi(g \pm \delta)$ (15), we find that near the critical point this condition implies that the system reaches the thermodynamic limit when

$$N|\delta| \gg 1, \quad (30)$$

which is numerically studied in Ref. [13]. It explains why the change of either N or δ can drive the system into the thermodynamic limit.

It is currently unknown how to find a closed-form expression for the product (29). Thus, we have to restore to approximations. We assume that $N \rightarrow \infty$ at the fixed δ , take the logarithm of Eq. (29), and then replace the sum over momenta with the integral (25).

Introducing the relative distance from the critical point

$$c = \frac{g-1}{|\delta|},$$

we obtain the following approximate result [13, 31]

$$\frac{\ln F(g, \delta)}{N} \simeq -|\delta|A(c), \quad (31)$$

where

$$A(c) = \begin{cases} \frac{1}{4} + \frac{|c|K(c_1)}{4} + \frac{(|c|-1)\text{Im}E(c_2)}{4\pi} & \text{for } |c| < 1, \\ \frac{|c|}{4} - \frac{|c|K(c_1)}{2\pi} - \frac{(|c|-1)\text{Im}E(c_2)}{4\pi} & \text{for } |c| \geq 1, \end{cases} \quad (32)$$

$$c_1 = -4\frac{|c|}{(|c|-1)^2}, \quad c_2 = \frac{(|c|+1)^2}{(|c|-1)^2}.$$

The complete elliptic integrals of the first and second kind are defined as

$$K(x) = \int_0^{\pi/2} \frac{d\phi}{\sqrt{1-x\sin^2(\phi)}}, \quad E(x) = \int_0^{\pi/2} d\phi \sqrt{1-x\sin^2(\phi)},$$

respectively. Several remarks are in order now.

First, Eq. (31) provides the leading order term of the $N \rightarrow \infty$ expansion of the exact expression for fidelity per lattice site, i.e., $-\ln F(g, \delta)/N$. Its accuracy is illustrated in Fig. 5. The next order correction to fidelity per lattice site is discussed in Ref. [31], where we refer the reader for the details. It comes from the difference between the sum and the integral:

$$\sum_{k=\pi/N}^{\pi-\pi/N} \ln \cos\left(\frac{\theta_+(k) - \theta_-(k)}{2}\right) - \frac{N}{2\pi} \int_0^\pi dk \ln \cos\left(\frac{\theta_+(k) - \theta_-(k)}{2}\right). \quad (33)$$

In particular, the next order approximation to $\ln F(g, \delta)/N$ at the quantum critical point $g_c = 1$ is

$$\frac{\ln F(1, \delta)}{N} \simeq -\frac{|\delta|}{4} + \frac{\ln(2)}{2N}, \quad (34)$$

where the $\ln(2)/2$ prefactor of the subleading term comes from the evaluation of Eq. (33) in the $N \rightarrow \infty$ limit [31]. We will show in Sec. V that the subleading term can be accurately extracted out from the probability of finding the system in the ground state after the non-equilibrium quantum phase transition.

Second, it should be stressed that Eq. (31) is derived for $|\delta| \ll 1$ and $|g-1| = |c\delta| \ll 1$. This is sufficient for describing the sharp drop of fidelity in the vicinity of the critical point. It should be noticed that fidelity in the thermodynamic limit can change by several orders of magnitude around the critical point when the magnetic field is changed by a few δ 's. Note that this observation holds for $1/N \ll |\delta| \ll 1$, so fidelity is indeed a sensitive probe of quantum criticality!

Third, Eq. (31) analytically shows how the Anderson orthogonality catastrophe happens in the quantum Ising model. It proves that the overlap between the Ising model ground states in the quantum critical region is exponentially small in the system size in the thermodynamic limit.

Fourth, the expression for $A(c)$ can be simplified for $|c| \gg 1$. Indeed, one finds that $A(c)$ approaches $1/16|c|$ in this limit (Fig. 5). This leads to the following approximation

$$F(g, \delta) \simeq \exp\left(-\frac{N\delta^2}{16|g-1|}\right). \quad (35)$$

If additionally $-N\delta^2/16|g-1| \ll 1$, then this expression yields the same result as Eq. (2). Finally, we note that the solutions (31) and (35) agree with the scaling results (6) and (7), respectively.

V. DYNAMICS OF QUANTUM PHASE TRANSITIONS

We will discuss now what insights into the dynamics of the quantum quench are provided by fidelity. Although the discussion below is based on Sec. V of Ref. [31], the numerical results presented here have not been published before. We focus here on the dynamics of the quantum Ising chain, but the discussion can be easily generalized to other ‘‘typical’’ quantum critical systems (see the end of this section).

To start, we consider an instantaneous quench, i.e., a sudden change of the parameter g of the Hamiltonian (8) from g_1 to g_2 . If the system was initially prepared in the ground state $|g_1\rangle$, then the probability of finding it in the ground state after the quench equals

$$|\langle g_1 | g_2 \rangle|^2 = F^2(g, \delta), \quad g = \frac{g_1 + g_2}{2}, \quad \delta = \frac{g_2 - g_1}{2},$$

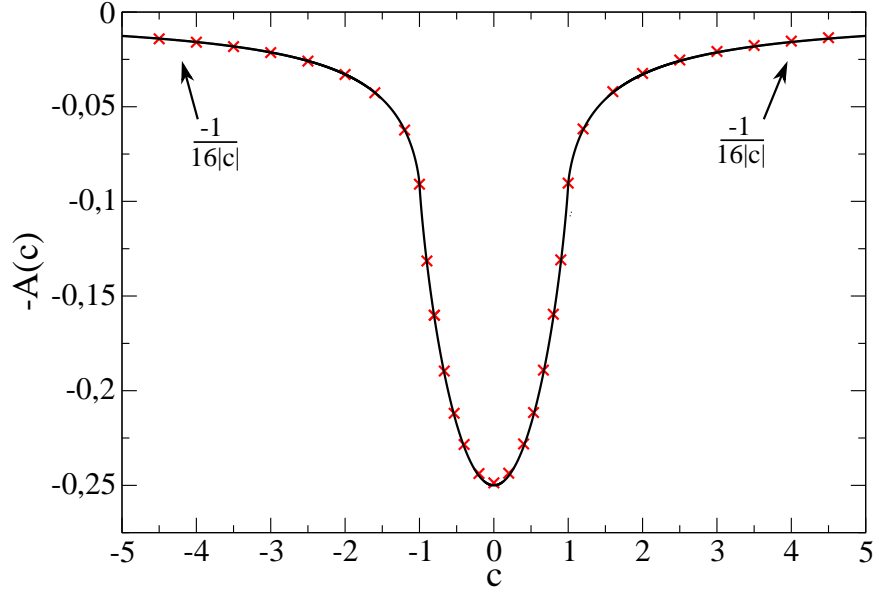


Figure 5: The scaling function $A(c)$ (32). Black line shows $-A(c)$ while the red crosses show $\ln F(1 + c|\delta|, \delta) / N|\delta|$, where $N = 10^5$ and $\delta = \pi/1000$. Note that the thermodynamic limit condition is well-reached for such a system as $N|\delta| = 100\pi \gg 1$. Adapted from Ref. [13].

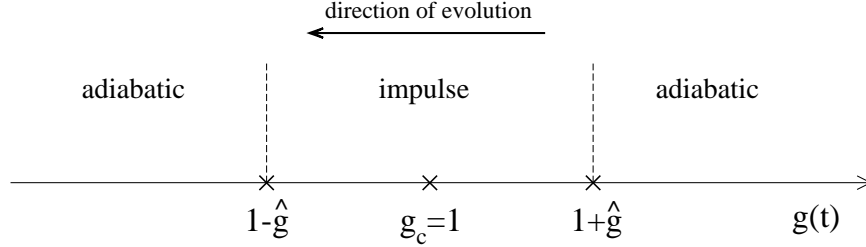


Figure 6: Illustration of the adiabatic-impulse approximation in the quantum Ising chain.

where $F(g, \delta)$ is given by Eq. (29) and the approximations discussed in Secs. III and IV can be used in the appropriate parameter ranges.

A much more interesting quench dynamics shows when the magnetic field is continuously changed in time

$$g(t) = -\frac{t}{\tau_Q}, \quad (36)$$

where $t : -\infty \rightarrow 0$ and the quench time τ_Q controls the speed of the driving. The dynamics of the Ising chain due to such time variation of the magnetic field is exactly solved in Ref. [32] (see Refs. [33] and [34] for the recent reviews of the dynamics of quantum phase transitions). We will now link fidelity to the probability of finding the system in the ground state after such a quench. To do so, we invoke the quantum version of the adiabatic-impulse approximation discussed in Ref. [35] (see also Ref. [36]). This approximation splits the evolution across the critical point into three parts depicted in Fig. 6:

- The first adiabatic regime takes place when the system is far away from the critical point, say

$$g(t) > 1 + \hat{g},$$

where \hat{g} will be discussed below. It is assumed in this regime that the system's wave-function $|\psi(t)\rangle \simeq e^{i\phi(t)}|g(t)\rangle$, where $|g(t)\rangle$ denotes the instantaneous ground state of $\hat{H}(g(t))$ (8) and $\phi(t)$ is the global phase. Such dynamics is possible when the gap in the excitation spectrum is large enough.

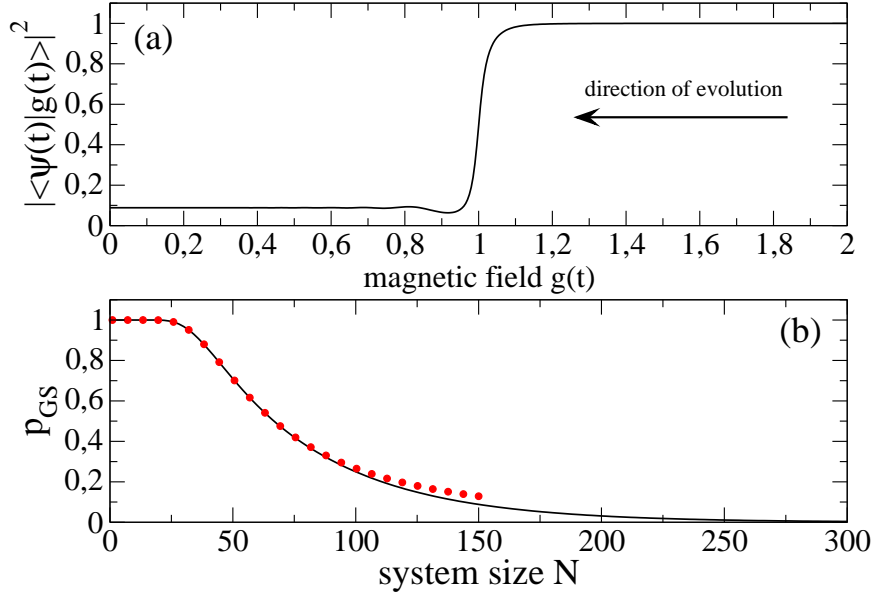


Figure 7: Panel (a): the probability of finding the $N = 150$ Ising chain in the *instantaneous* ground state during a quench. Panel (b): the probability p_{GS} of finding the Ising chain in the ground state by the *end* of time evolution. The quench protocol in both panels is provided by Eq. (36) with $\tau_Q = 50$. The evolution starts from the paramagnetic phase ground state at the magnetic field $g(t = -5\tau_Q) = 5$ and it ends in the ferromagnetic phase at the magnetic field $g(t = 0) = 0$. The solid line on both panels is a numerical calculation. The red dashed-dotted line in the lower panel shows $1 - \exp(-2\pi^3\tau_Q/N^2)$. It illustrates what happens when the finite-size effects play a role [39].

- The impulse regime happens around the critical point,

$$|g(t) - 1| < \hat{g},$$

and the wave-function, apart from the overall phase factor, is assumed to be constant: $|\psi(t)\rangle \simeq e^{i\phi(t)}|1 + \hat{g}\rangle$. This happens when the gap in the excitation spectrum becomes too small to support adiabatic dynamics *at the given quench time*.

- The second adiabatic regime happens when

$$g(t) < 1 - \hat{g},$$

where it is assumed that no additional excitations are created by the quench, i.e., $|\langle g(t)|\psi(t)\rangle| = \text{const.}$

These three stages of evolution are easily seen on Fig. 7a, where the squared overlap of the wave function $|\psi(t)\rangle$ onto the instantaneous ground state $|g(t)\rangle$ of the Hamiltonian (8) is plotted for a typical time evolution. We mention in passing that we have done the numerics for this section in the same way as in our recent Ref. [37] discussing the counterdiabatic dynamics of the Ising chain [38].

The size of the impulse regime is governed by the gap in the excitation spectrum and the rate of driving. It is estimated by solving the following equation (see e.g. Refs. [35], [36], and [40] for different versions of this simple estimation and the physical reasons supporting it)

$$\frac{1}{\text{gap}(1 \pm \hat{g})} \sim \frac{\text{gap}}{\frac{d}{dt}\text{gap}} \Big|_{g=1 \pm \hat{g}}.$$

Assuming that the system is infinite, the relevant energy gap in the quantum Ising model is given here by $2|g - 1|$ for $g \geq 0$ that we consider in this section. This gives us

$$\hat{g} \sim \frac{1}{\sqrt{\tau_Q}}. \quad (37)$$

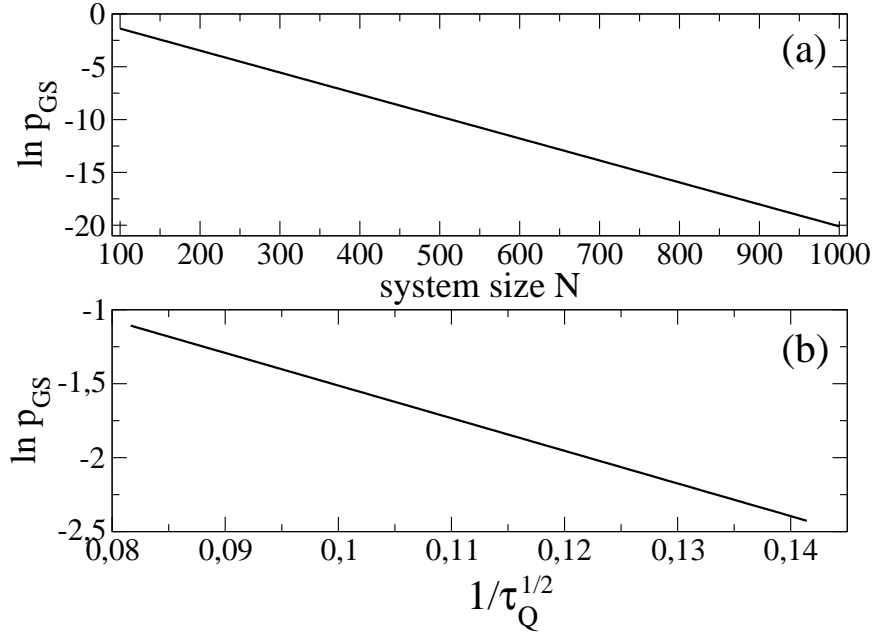


Figure 8: Logarithm of the probability of finding the Ising chain in the ground state after the quench; see the discussion around Eq. (42) for the details.

It should be stressed that there is no sharp splitting between the adiabatic and impulse dynamics. Instead, there is a crossover and Eq. (37) provides the scaling of its location with the quench time τ_Q . Such estimation is meaningful for slow quenches only, $\tau_Q \gg 1$, which can be numerically checked.

The quench time, however, cannot be too large in a finite Ising chain if we want to see the impulse regime. Indeed, given the fact that the gap at the critical point scales as $1/N$, one can always drive the system so slow that it will adiabatically cross the critical point (its excitation will be then exponentially small in the quench time [39], which we illustrate in Fig. 7b). Note that the gap in this section refers to the difference between the eigenenergy of the ground state and the lowest excited state that can be populated during the evolution. It shall not be confused with the gap between the positive and negative parity subspaces studied in Sec. II; the parity is conserved during the time evolution.

We expect that the finite-size effects are negligible during a non-equilibrium quench, when the spin-spin correlations in the system's wave-function $|\psi(t)\rangle$ decay on a length scale much smaller than the system size. Within the adiabatic-impulse approximation this length scale is upper bounded by the equilibrium correlation length (15) taken at $1 + \hat{g}$. Thus, it is reasonable to expect that the finite-size effects are negligible when

$$N \gg \xi(1 + \hat{g}) \sim \sqrt{\tau_Q}, \quad (38)$$

which we assume below. This educated guess is rigorously discussed in Refs. [32] and [39].

Using the adiabatic-impulse approximation, we estimate that the probability p_{GS} of finding the system in the instantaneous ground state away from the critical point, i.e., when $|g - 1| \gg \hat{g}$, is

$$p_{GS} = |\langle 1 - \hat{g} | 1 + \hat{g} \rangle|^2 = F^2(1, \delta), \quad (39)$$

$$\delta = \hat{g} \sim \frac{1}{\sqrt{\tau_Q}}. \quad (40)$$

Combining Eqs. (38) and (40), we see that the condition (30) is satisfied. Therefore, the thermodynamic expression (34) for fidelity should be used in Eq. (39), which leads us to

$$p_{GS} = 2 \exp\left(-N \times \frac{\text{const}}{\sqrt{\tau_Q}}\right), \quad (41)$$

where the prefactor of 2 comes from the subleading term in Eq. (34).

This simple prediction can be compared to numerics. To do so, we employ the quench protocol (36). The evolution starts from the paramagnetic phase ground state at the magnetic field $g(t = -5\tau_Q) = 5$ and it ends in the ferromagnetic phase at $g(t = 0) = 0$. To simplify the comparison between the theory and numerics, we take the logarithm of Eq. (41) getting

$$\begin{aligned}\ln(p_{GS}) &= \ln(2) - N \times \frac{\text{const}}{\sqrt{\tau_Q}}, \\ \ln(2) &= 0.693147\dots\end{aligned}\tag{42}$$

First, we choose the quench time $\tau_Q = 50$ and change the system size N in the range $[100, 1000]$. The standard linear fit to the numerics from Fig. 8a yields:

$$\ln(p_{GS}) = 0.693146(1) - 0.020800730(1)N.$$

The linear dependance of $\ln(p_{GS})$ on the system size N is nicely confirmed by the fit, and we note that the fitted intercept surprisingly well agrees with the theoretical one.

Second, the system size is set to $N = 150$ and the quench time τ_Q is varied in the range $[50, 150]$. The linear fit to the numerics from Fig. 8b gives

$$\ln(p_{GS}) = 0.6940(1) - \frac{22.065(1)}{\sqrt{\tau_Q}}.$$

The intercept again agrees surprisingly well with the theoretical prediction and the linearity of $\ln(p_{GS})$ in the inverse square root of the quench time is nicely confirmed.

The fitted lines are not depicted on Figs. 8a and 8b because they are practically indistinguishable from the numerics. It is worth to stress that for the system sizes considered in these numerical studies the inclusion of the subleading term to fidelity per lattice site (34) is crucial for getting a good agreement between the theoretical prediction for p_{GS} and numerics.

Finally, we mention that a more general result can be obtained if we assume that the gap closes at the critical point in the infinite system as $|g - g_c|^{z\nu}$, where z and ν are the universal critical exponents. Repeating the steps outlined above one gets [31]

$$p_{GS} \sim \exp\left(-N \times \frac{\text{const}}{\tau_Q^{d\nu/(1+z\nu)}}\right),\tag{43}$$

where d stands for the dimensionality of the system. The Ising result is recovered for $z = \nu = d = 1$.

The results (41) and (43) have simple interpretation in the context of symmetry breaking phase transitions, which in the quantum Ising model happen when the system is driven from the paramagnetic to the ferromagnetic phase. As predicted by the Kibble-Zurek theory [41], such transitions lead to the creation of topological defects whose density scales with the quench time as $1/\tau_Q^{d\nu/(1+z\nu)}$. Thus, the probability of finding the system after the quench in its instantaneous ground state is exponential in the number of topological defects created during the non-adiabatic crossing of the quantum critical point.

VI. FIDELITY IN CENTRAL SPIN SYSTEMS

It turns out that knowledge of fidelity helps in the studies of the central spin-1/2 coupled to the Ising chain [42, 43]. The Hamiltonian of such a system reads

$$\hat{H}(g) - \delta \sum_{j=1}^N \sigma_j^z \sigma_S^z,$$

where $\hat{H}(g)$ is given by Eq. (8), σ_S^z is the Pauli matrix of the central spin, and δ is the central spin–environment coupling. Such a model is known as the central spin model because of the uniform coupling of the central spin to its “environment”. Without going into details, we will mention two problems, where the expressions for fidelity from Secs. III and IV can be used.

Critical dynamics of decoherence. Suppose that the magnetic field is quenched by the protocol (36). The system is initially in the product state

$$(c_+ |\uparrow\rangle + c_- |\downarrow\rangle) \otimes |g(t = -\infty)\rangle, \quad (44)$$

where the central spin is in an arbitrary superposition of its up/down states and the Ising chain is in the ground state $|g\rangle$ of $\hat{H}(g)$. The idea now is to study the decoherence of the central spin due to the presence of the many-body Ising environment undergoing a non-equilibrium quench across the critical point(s). As is explained in Ref. [42], the knowledge of fidelity $F(g, \delta)$ is crucial for the explanation of the decoherence rate of the central spin in this non-equilibrium system.

Magnetic Schrödinger's cats. We consider now the same system as the one described above and assume that the Ising chain is adiabatically driven towards the critical point, where the time variation of the magnetic field (36) stops. Assuming that the evolution starts from the initial state (44) and that $\tau_Q \gg N^2$, the final state of the system will be approximately given by

$$c_- e^{i\phi_-} |\downarrow\rangle \otimes |g - \delta\rangle + c_+ e^{i\phi_+} |\uparrow\rangle \otimes |g + \delta\rangle,$$

where ϕ_{\pm} stand for the phases picked by the system during the evolution [43]. Assuming that $g - \delta < g_c < g + \delta$, $|g - \delta\rangle$ and $|g + \delta\rangle$ are the ferromagnetic and paramagnetic ground states of the Ising Hamiltonian. This state is the magnetic Schrödinger's cat state. The dead/alive cat states are the ferromagnetic/paramagnetic ground states. The state of the radioactive atom that has/has not decayed is played by the up/down states of the central spin. It is not, however, the ordinary Schrödinger's cat because the two cat states are not orthogonal,

$$|\langle g - \delta | g + \delta \rangle| = F(g, \delta) \neq 0.$$

It would be now certainly interesting to understand how the rate of decoherence of such a superposition state depends on the similarity between the two cat states, i.e., their fidelity. It is perhaps worth to stress that the experimental studies of the decoherence of "simpler" superpositions have been recognized [44, 45] by the Nobel committee in 2012, so it would be certainly very exciting to experimentally quantify the decoherence rate of the magnetic Schrödinger's cats! For other applications of fidelity in this context see Ref. [43]. For similar ideas in the cold ion and cold atom systems see Refs. [46] and [47], respectively.

VII. SUMMARY

We finish these lecture notes by quoting P. W. Anderson [12] "*While wave functions and overlap integrals are often of little consequence in many-body systems, this one is at least related to the response to a sudden application of the potential, and indicates that response involves only the emission of low-energy excitations into the continuum, as well as that the truly adiabatic application of such a potential to such a system is impossible*". We hope that these lecture notes provide further evidence that the wave functions and overlap integrals are indeed very useful in the studies of many-body quantum systems.

Acknowledgments

This work has been supported by the Polish National Science Centre (NCN) grant DEC-2013/09/B/ST3/00239. I would like to thank Marek Rams for the collaboration on the topics discussed in these lecture notes and for insightful comments about this manuscript.

-
- [1] S. Sachdev, *Quantum Phase Transitions* (Cambridge University Press, Cambridge, 2011).
 - [2] S. Sachdev and B. Keimer, *Phys. Today* **64**, 29 (2011).
 - [3] P. Zanardi and N. Paunković, *Phys. Rev. E* **74**, 031123 (2006).
 - [4] S.-J. Gu, *Int. J. Mod. Phys. B* **24**, 4371 (2010).
 - [5] M. A. Continentino, *Quantum Scaling in Many-Body Systems* (World Scientific Publishing, Singapore, 2001).
 - [6] A. F. Albuquerque, F. Alet, C. Sire, and S. Capponi, *Phys. Rev. B* **81**, 064418 (2010).
 - [7] V. Gritsev and A. Polkovnikov, in *Understanding in Quantum Phase Transitions* edited by L. Carr (Taylor & Francis, Boca Raton, 2010).

- [8] P. Zanardi, P. Giorda, and M. Cozzini, *Phys. Rev. Lett.* **99**, 100603 (2007).
- [9] L. C. Venuti and P. Zanardi, *Phys. Rev. Lett.* **99**, 095701 (2007).
- [10] M. Kolodrubetz, V. Gritsev, and A. Polkovnikov, *Phys. Rev. B* **88**, 064304 (2013).
- [11] S.-J. Gu and W. C. Yu, *Europhys. Lett.* **108**, 20002 (2014).
- [12] P. W. Anderson, *Phys. Rev. Lett.* **18**, 1049 (1967).
- [13] M. M. Rams and B. Damski, *Phys. Rev. Lett.* **106**, 055701 (2011).
- [14] H.-Q. Zhou and J. P. Barjaktarevič, *J. Phys. A* **41**, 412001 (2008).
- [15] H.-Q. Zhou, J.-H. Zhao, and B. Li, *J. Phys. A* **41**, 492002 (2008).
- [16] R. Coldea *et al.*, *Science* **327**, 177 (2010).
- [17] K. Kim *et al.*, *New J. Phys.* **13**, 105003 (2011); S. Korenblit *et al.*, *New J. Phys.* **14**, 095024 (2012); R. Islam *et al.*, *Science* **340**, 583 (2013); P. Richerme, C. Senko, J. Smith, A. Lee, S. Korenblit, and C. Monroe, *Phys. Rev. A* **88**, 012334 (2013).
- [18] B. P. Lanyon *et al.*, *Science* **334**, 57 (2011).
- [19] J. Simon, W. S. Bakr, R. Ma, M. E. Tai, P. M. Preiss, and M. Greiner, *Nature* **472**, 307 (2011).
- [20] Z. Li *et al.*, *Phys. Rev. Lett.* **112**, 220501 (2014).
- [21] E. Lieb and T. Schultz, and D. Mattis, *Ann. Phys. (N.Y.)* **16**, 407 (1961).
- [22] P. Pfeuty, *Ann. Phys.* **57**, 79 (1970).
- [23] E. Barouch and B. M. McCoy, *Phys. Rev. A* **3**, 786 (1971).
- [24] B. Damski and M. M. Rams, *J. Phys. A* **47**, 025303 (2014).
- [25] A. De Pasquale and P. Facchi, *Phys. Rev. A* **80**, 032102 (2009).
- [26] B. Damski, *Phys. Rev. E* **87**, 052131 (2013).
- [27] E. Barouch and B. M. McCoy, *Phys. Rev. A* **3**, 786 (1971).
- [28] E. Fradkin and L. Susskind, *Phys. Rev D* **17**, 2637 (1978).
- [29] E. T. Whittaker and G. N. Watson, *A Course of Modern Analysis* (Cambridge University Press, 4th Edition).
- [30] P. Zanardi, M. G. A. Paris, and L. C. Venuti, *Phys. Rev. A* **78**, 042105 (2008).
- [31] M. M. Rams and B. Damski, *Phys. Rev. A* **84**, 032324 (2011).
- [32] J. Dziarmaga, *Phys. Rev. Lett.* **95**, 245701 (2005).
- [33] J. Dziarmaga, *Adv. Phys.* **59**, 1063 (2010).
- [34] A. Polkovnikov, K. Sengupta, A. Silva, and M. Vengalattore, *Rev. Mod. Phys.* **83**, 863 (2011).
- [35] B. Damski, *Phys. Rev. Lett.* **95**, 035701 (2005).
- [36] W. H. Zurek, U. Dorner, and P. Zoller, *Phys. Rev. Lett.* **95**, 105701 (2005).
- [37] B. Damski, *J. Stat. Mech.* (2014) P12019.
- [38] A. del Campo, M. M. Rams, and W. H. Zurek, *Phys. Rev. Lett.* **109**, 115703 (2012).
- [39] L. Cincio, J. Dziarmaga, J. Meisner, and M. M. Rams, *Phys. Rev. B* **79**, 094421 (2009).
- [40] B. Damski and W. H. Zurek, *Phys. Rev. Lett.* **99**, 130402 (2007).
- [41] A. del Campo and W. H. Zurek, *Int. J. Mod. Phys. A* **29**, 1430018 (2014).
- [42] B. Damski, H. T. Quan, and W. H. Zurek, *Phys. Rev. A* **83**, 062104 (2011).
- [43] M. M. Rams, M. Zwolak, and B. Damski, *Sci. Rep.* **2**, 655 (2012).
- [44] D. J. Wineland, *Rev. Mod. Phys.* **85**, 1103 (2013).
- [45] S. Haroche, *Rev. Mod. Phys.* **85**, 1083 (2013).
- [46] J. D. Baltrusch, C. Cormick, G. De Chiara, T. Calarco, and G. Morigi, *Phys. Rev. A* **84**, 063821 (2011).
- [47] C. Maschler and H. Ritsch, *Phys. Rev. Lett.* **95**, 260401 (2005).
- [48] Whenever $k = 0, \pi$, one should keep only the $K = +k$ term in the sum (12).